Local Condensation and Evaporation Heat Transfer Coefficient Measurements of Binary Mixture Refrigerant R454B Inside a Plate Heat Exchanger

Md. Mahbubur Rahman^{1,2,*}, Afnan Hasan^{1,3}, Djiby Bal¹, Keishi Kariya⁴ and Akio Miyara^{4,5}

¹Graduate School of Science and Engineering, Saga University, Saga 840-8502, Japan

²Department of Mechanical Engineering, Khulna University of Engineering & Technology, Khulna 9203, Bangladesh

³Department of Mechanical Engineering, Chittagong University of Engineering & Technology, Chattogram 4349, Bangladesh

⁴Department of Mechanical Engineering, Saga University, Saga 840-8502, Japan

⁵International Institute for Carbon-Neutral Energy Research, Kyushu University, Fukuoka 819-0395, Japan

ABSTRACT

This paper explores the evaluation of the local heat transfer coefficient of a binary mixture refrigerant R454B experimentally in a vertical brazed plate heat exchanger during both condensation and evaporation. The experiments were carried out at different mass fluxes of 10 kg/m²s and 50 kg/m²s in a specially designed test section. This test section incorporates eight stainless steel plates: two chevron plates processed at 60° for the refrigerant flow channel, two flat plates for heat transfer, and four plates dedicated to water flow channels on both sides of the refrigerant channel. The refrigerant and water flow in a counter pattern, with the refrigerant centrally flowing between the two water channels on the outer sides. To measure wall surface temperatures near the refrigerant and water sides, 20 thermocouples were strategically placed within the test section. The local heat transfer coefficients were calculated using wall temperatures from the refrigerant side, refrigerant saturation temperature, and local heat flux under downward flow condition during condensation and upward flow condition during evaporation experiments. The experimental measurement results showed that local heat transfer coefficients decreases with increase of wetness during condensation and local heat transfer coefficient increases with the increase of vapor quality during evaporation with different values in horizontal direction inside the plate heat exchanger.

Keywords: Plate heat exchanger, heat transfer, evaporation, condensation and mixture refrigerant

1. INTRODUCTION

Plate Heat Exchangers (PHEs) find extensive use across various industrial sectors such as dairy, processing, paper production, refrigeration, heating, ventilation, and air conditioning. Their superiority over other heat exchanger types stems from several factors. PHEs excel in saving energy and space due to their higher ratio of heat transfer area to volume. They're lightweight, feature flexible designs, and boast high thermal efficiencies. Their adaptable design provides a significant edge when modifying the heat transfer area; adding or removing plates can be done seamlessly without disrupting pipe connections.

The European Union has set in motion a plan to gradually eliminate refrigerants with higher Global Warming Potential (GWP), especially in portable air conditioners and household refrigerators/freezers, following regulations in EU No. 517/2014. This has led to increased interest in alternative refrigerants that boast low GWP and zero Ozone Depletion Potential (ODP). However, these low GWP refrigerants often come with elevated costs and greater energy consumption. To address this challenge, exploring blended refrigerants that meet acceptable criteria has emerged as a potential solution. Researchers are actively seeking alternatives that exhibit both low GWP and comparable heat transfer properties. While prior studies extensively investigated the heat transfer characteristics of various refrigerants in plate heat exchangers during condensation and evaporation, most focused on overall heat transfer traits [1]-[14], with only a of local heat transfer within plate heat exchangers. Sarraf et al.[19] utilized Infrared Thermography (IR) to ascertain local heat transfer coefficients in a prototype brazed plate heat exchanger (BPHE) during the complete condensation of R601. Through infrared thermography, they identified the global and local thermo-hydraulic features of the PHE, including vapor quality, heat flux density, and heat transfer coefficient. Their investigation also delved into the influence of mass flux on these properties. Wang and Kabelac [20] conducted experimental research on the quasi-local heat transfer characteristics of R1234ze(E) and R134a within a microstructured plate heat exchanger. Their study focused on analyzing the impact of refrigerant mass flux and saturation temperature on condensation heat transfer. Additionally, they drew conclusions regarding transitions observed in vapor quality, demonstrating shifts from laminar flow to turbulent flow and illustrating film condensation phenomena. Longo et al. [22] similarly explored the local heat transfer coefficients of R32 and R410A within a BPHE. Their study centered on identifying a transition concerning mass flux, moving from gravity-controlled condensation to forced convection condensation. The local heat transfer coefficient fluctuates not just along the flow direction but also across the width due to gas-liquid distribution [23]-[25]. Variations in refrigerant distribution at the inlet and outlet lead to maldistribution, affecting local condensation heat transfer within a plate heat exchanger [22]. The presence of different boiling mechanisms in the liquid-preferred and vapor-preferred paths induces alterations in local evaporation heat transfer within plate heat exchanger [18].

limited number [15]-[22] exploring the specific intricacies

^{*} Corresponding author's email: mahbub rahman@me.kuet.ac.bd

Since the research work about local heat transfer coefficient is scarce, to gain deeper insights into heat transfer behaviors, detailed knowledge about local heat transfer becomes imperative. However, measurements of local wall temperatures and heat fluxes are difficult because of the complicated structure. A specially designed test section has been constructed for the measurement of heat transfer coefficient of a zeotropic mixture refrigerant R454B in the present study. The physiochemical properties of the refrigerant are shown in Table 1.

Table 1 Physiochemical properties of R454B

Refrigerant	R454B	
Composition mass percentage	R32 68.9%	
	R1234yf 31.1%	
Temperature glide (°C)	1.5	
ASHRAE Safety class	A2L	
GWP	467	
ODP	0	
Molar weight (kg/kmol)	62.6	
Normal boiling point (°C)	-50.73	
Critical pressure (kPa)	5041	
Critical temperature (°C)	77.0	
Liquid density(kg/m ³)	1001	
Temperature glide (°C)	1.5	
Liquid thermal conductivity	105.4	
$(mW/m\cdot K)$		
Vaporisation enthalpy (kJ/kg)	227.51	

The findings in the present study will help to better understand the local heat transfer phenomena inside the plate heat exchanger.

2. EXPERIMENTAL SETUP AND PROCEDURES

2.1 Refrigerant loop

The experimental setup in the present study consists of five

different loops and a data acquisition system for the investigation of local heat transfer of the mixture refrigerant R454B in a vertical brazed plate heat exchanger [26]. They have a refrigerant loop shown in Figure 1, three water loops for preheater, test section and condenser and a cold-water brine loop for the subcooler. The refrigerant loop is the primary loop of the experimental setup. For attaining various experimental conditions, it is needed to control the flow and temperature in the other four loops.

The refrigerant loop comprises a setup of a magnetic pump, a refrigerant mass flow meter, a preheater, a test section "the plate heat exchanger", a condenser, a subcooler, three mixing chambers and three sight glasses. A magnetic pump circulates the refrigerant in the whole loop. A mass flow meter is positioned between the pump and the preheater to control the flow rate of the refrigerant. The preheater transfers heat from the water to the refrigerant to reach a specific vapor quality at the inlet of the test section. The vapor of a certain quality then entered the test section and the refrigerant R454B condensed (in condensation experiment) or evaporated (in boiling experiment) there. The vapor-liquid two-phase refrigerant from the outlet of the test section is finally condensed in the condenser. Then the refrigerant is subcooled by controlling the flow rate of a low-temperature water brine mixture in the subcooler. The system pressure of the refrigerant loop can be controlled by adjusting the temperature in the condenser. The purpose of the filter was to remove any solid particles that may have been present in the loop. The refrigerant coming from the exit of the test section was maintained in a subcooled condition to prevent cavitation at the pump inlet [27].

2.2 Test section

Eight stainless steel plates (material SUS303) were brazed together to form the specifically designed test section that

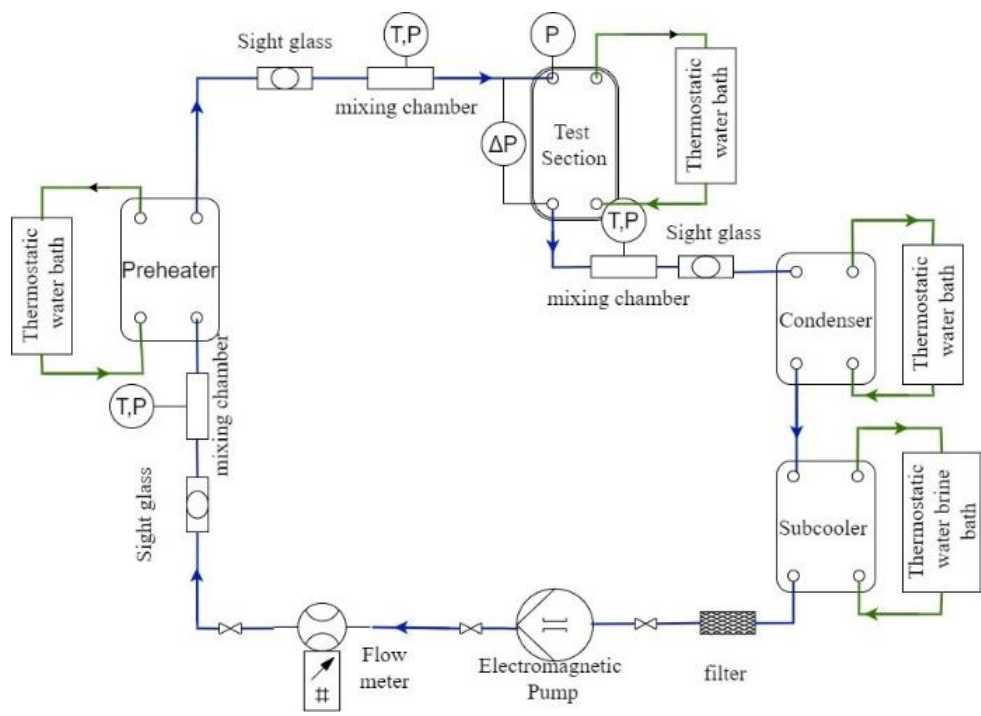


Figure 1: Refrigerant flow loop of experimental setup[27]

was utilized in this study. Among two of them were processed chevron plates of angle 60° .

The flow of the refrigerant occurs in the channel created by the space between these two chevron plates. Two flat plates were set for heat transfer measurements next to the chevron-shaped plates. The other four plates were dedicated to forming two water flow channels. Figure 2a represents a detailed view of thermocouple measurement points and the flow of water and refrigerants in the cross-section of the test plate. The red and blue regions, shown in Figure 2b, indicate, respectively, the refrigerant and cooling water channels. Table 2shows the geometrical characteristics of the test section with the geometrical attributes shown in Figure 3.

2.3 Experimental procedures

Prior to conducting each experiment, the setup's system pressure is first maintained at a predetermined level through adjusting the condenser's temperature. The hot water loop for the preheater's temperature and flow rate are then modified to achieve the required vapor quality of R454B at the test section's inlet. Changing the temperature and flow rate of the water loop for the test section allows for adjustment of the heat transfer rate between the counter flow channels in the test section. Any modification to the system variables causes a change in the flow's temperature and pressure. A statistically steady state condition can be reached in between 20 and 100 minutes. The data acquisition device is subsequently turned on, and in the following 40 seconds, it scans each data channel ten times.

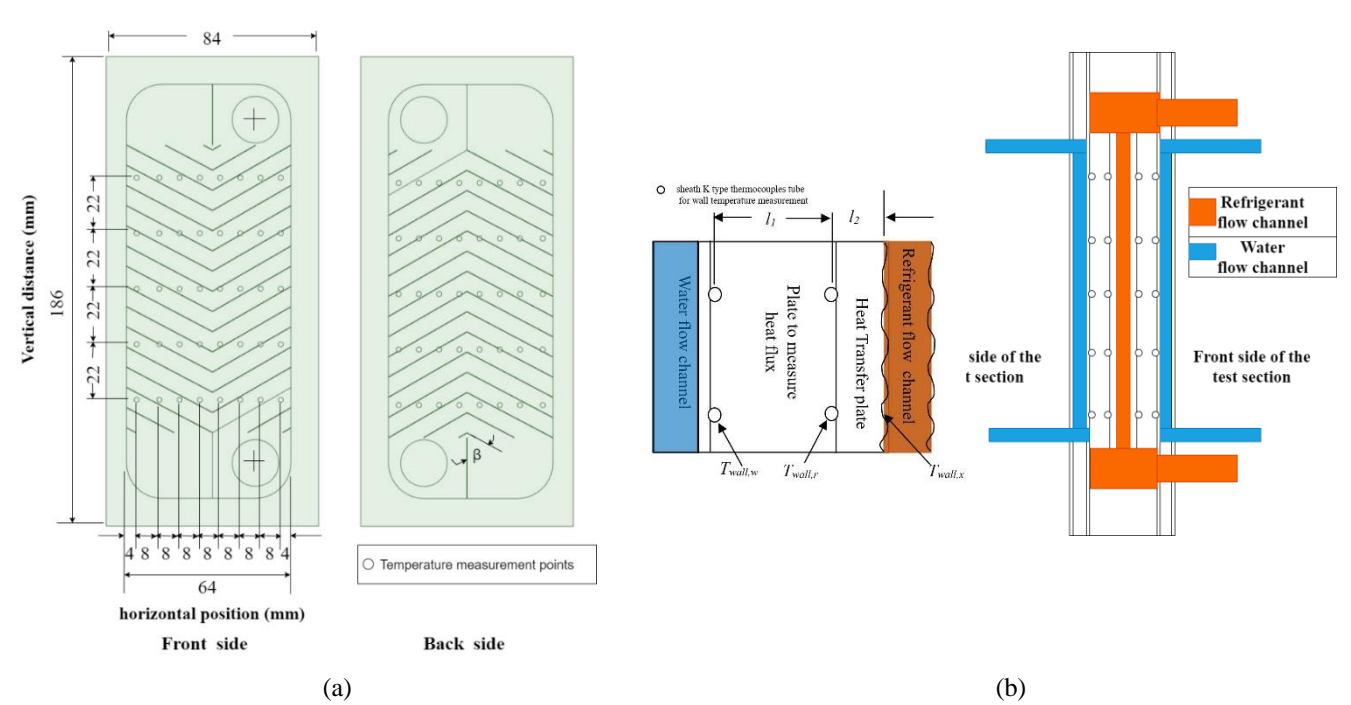


Figure 2: Details of (a) measurement positions and (b) flow directions [27]

Table 2:Geometrical characteristics of the test section [28]

Parameters	Value
Fluid Flow plate length, L (mm)	117.5
Plate width, W (mm)	64
Plate thickness (mm)	5
Area of the plate (m ²)	0.0075
Corrugation type	Chevron
Chevron angle, $\beta(^0)$	60
Corrugation pitch, P(mm)	5.6
Corrugation depth, b(mm)	1.5
Number of plates	8
Number of channels on the refrigerant side	1
Number of channels on the water side	2
Thermal conductivity of the plate (W/m·K)	16.7

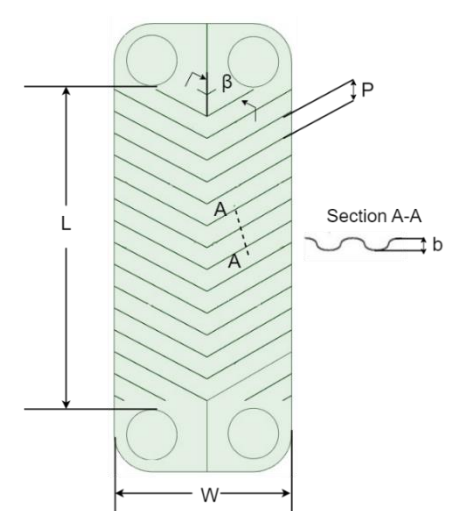


Figure 3: Geometrical attributes of the chevron plate

3. DATA REDUCTION

3.1 Local heat transfer coefficient

By assuming the steady state one dimensional heat conduction, the local heat flux q_x can be estimated from wall temperatures near refrigerant side $(T_{wall,r})$ and water side $(T_{wall,w})$ and thermal conductivity (λ_p) of the

plate shown in Eq. (1)
$$q_x = \lambda_p \left(\frac{T_{wall,r} - T_{wall,w}}{l_1} \right)$$
 (1)

 l_1 is the distance between thermocouples. The wall surface temperature of refrigerant side $T_{wall,x}$ can be calculated assuming linear temperature distribution as Eq.(2)

$$T_{wall,x} = T_{wall,r} \pm \left(\frac{q_x l_2}{\lambda}\right)$$
 (2)
'+' sign is for condensation and '-' sign is for evaporation.

l₂ is the distance between thermocouple and wall surface. The local heat transfer coefficient (LHTC) α_x is determined from the difference between wall surface temperature and saturation temperature shown in Eq. (3)

$$\alpha_x = \frac{q_x}{T_{sat} \sim T_{wall,x}}$$

$$T_{sat} \text{ is the saturation temperature of the working fluid side.}$$
(3)

3.2 Vapor quality

The local specific enthalpy (h_i) on the test plate is derived using the following procedure.

$$h = f(T, P) \tag{4}$$

The amount of heat exchange in the preheater $(Q_{w,pre})$ is calculated by Eq. (5):

$$Q_{w,pre} = m_w \left(h_{w,pre,out} - h_{w,pre,in} \right) \tag{5}$$

where \vec{m}_w is mass flow rate of water and $h_{w,pre,in}$ and $h_{w,pre,in}$ are the specific enthalpies of the preheater outlet and inlet of the water respectively.

The specific enthalpy at test section inlet $(h_{t,in})$ is obtained from the amount of heat exchange $(Q_{w,pre})$ for the preheater, mass flow rate $(\dot{m_r})$ of the refrigerant and heat loss (Q_{loss}) from the outlet of the preheater to the inlet of the test section.

$$h_{t,in} = h_{r,pre,in} + \frac{Q_{w,pre}}{\dot{m}_r} - \frac{Q_{loss}}{\dot{m}_r}$$
 (6)

The heat loss Q_{loss} is calculated from the steady state heat conduction equation of the multilayer cylinder.

The local specific enthalpy is calculated as follows.

$$h_i = h_{\rm t,in} \pm \frac{Q_i}{\dot{m}}$$

$$h_{i+1} = h_i \pm \frac{Q_{i+1}}{\dot{m}} \tag{7}$$

'+' sign is for evaporation and '-' sign is for condensation. the heat flow between two neighboring thermocouples obtained from the local heat flux q_x and the heat transfer area A_i.

$$Q_i = q_x A_i \tag{8}$$

 $Q_i = q_x A_i$ (8) The local vapor quality (x_i) is determined from specific

$$x_i = \frac{h_i - h_l}{h_v - h_l} \tag{9}$$

 h_l and h_v are the specific enthalpies of saturated liquid and saturation vapor respectively.

Since mixture refrigerant R454B is azeotropic binary mixture of R32 and R1234yf with 68.9% and 31.1 % by mass respectively, the local refrigerant saturation temperatures are calculated by the mixture component mass balance.

$$\dot{m}_b w_b = \dot{m}_V w_V + \dot{m}_l w_l \tag{10}$$

 $\dot{m}_b, \ \dot{m}_l, \ \dot{m}_V$ represent the total mass flow rate, liquid phase mass flow rate and the vapor phase mass flow rate respectively.

As thermodynamic vapor quality is also defined as

$$x = \frac{\dot{m}_V}{\dot{m}_b} \tag{11}$$

From Eq. (10) and Eq. (11) the following relationship can

$$w_L = \frac{w_b}{1 + x\left(\frac{w_V}{w_L} - 1\right)} \tag{12}$$

 w_b , w_L and w_V are the bulk mass fraction, liquid phase mass fraction and vapor phase mass fraction of the binary mixture, respectively.

The bulk concentration of the binary temperature under operational conditions can be determined by the use of gas chromatography.

The saturation temperature T_{sat} is calculated by REFPROP 10 [29] with the following relation as shown Eq. (13).

$$T_{sat} = f(w_l, P) \tag{13}$$

The corresponding enthalpy for liquid and vapor phase is also evaluated from REFPROP 10.0 [29] by the function of the concentration and the pressures at the measurement point.

$$h_l = f(w_l, P) \tag{14}$$

$$h_{v} = f(w_{v}, P) \tag{15}$$

3.3 Experimental uncertainty

The values of the experimental uncertainty are reported [23][28] for the heat transfer coefficient and the vapor quality within $\pm 12\%$ and $\pm 4.5\%$ respectively.

4. EXPERIMENTAL RESULTS AND DISCUSSIONS

The condensation and evaporation experiments in a brazed plate heat exchanger were conducted to determine the heat transfer coefficients (both local and average) for the mixed refrigerant R454B. The heat transfer coefficients at various measurement points along the horizontal distance were examined for both the front and back sides of the plates, which served as the refrigerant flow channel in the test section. The results illustrate the variation of local heat transfer coefficients with vapor quality under

different flow and thermal conditions. Additionally, the average heat transfer coefficients of the mixture refrigerant R454B were experimentally obtained and compared with those of R1234yf in the same test facility.

4.1 Local condensation and evaporation heat transfer coefficient measurement for mixture refrigerant R454B

The experiments for the condensation and evaporation heat transfer (HT) of R454B mixture refrigerant inside the plate heat exchanger were carried out in two different mass fluxes of $10~kg/m^2s$ and $50~kg/m^2s$. Table 3 represents the thermal conditions for condensation heat transfer experiment.

Table 3.Test condition for condensation HT experiment

	Mass	T_{sat}	Vapor	Heat Flux,
Refrigerant	Flux, G	[°C]	Quality	$q [kW/m^2]$
	[kg/m ² s]		[-]	
R454B	10	30	1.0-0.0	9.2-11.5
K434B	50	30	1.0-0.0	6.8-18.9

The thermal conditions for evaporation heat transfer have been shown in Table 4.

Table 4.Test condition for evaporation HT experiment

Refrigerant	Mass Flux, G [kg/m ² s]	T _{sat} [°C]	Vapor Quality [-]	Heat Flux, q [kW/m ²]
R454B	10	10	0.0-0.9	9.0-14.2
	50	10	0.0-1.0	15.3-40.2

Figure 4 and Figure 5 illustrate the variation of the local heat transfer coefficient (LHTC) in the horizontal direction of the plate for different vapor qualities within

the test section, along with the horizontal average heat transfer coefficient during the condensation of R454B in a plate heat exchanger for mass fluxes 10 kg/m²s and 50 kg/m²s respectively at saturation temperature of 30 °C. Moreover, Figure 6 and Figure 7 showcase the change in the local heat transfer coefficient (LHTC) in the horizontal direction of the plate for various vapor qualities within the test section, along with the horizontal average heat transfer coefficient during the evaporation of R454B in a plate heat exchanger for mass fluxes 10kg/m²s and 50 kg/m²s respectively at saturation temperature of 10 °C. From Figure 4(a), (b), (c), (d) and (e) and Figure 5(a), (b), (c), (d) and (e), in the course of the condensation process

of the mixed refrigerant R454B in the plate heat exchanger, at mass fluxes of 10 kg/m²s and 50 kg/m²s, the local condensation heat transfer coefficient within the plate exhibits variability both in horizontal positions and vapor quality along the vertical distance of the Plate Heat Exchanger (PHE). The differences between the front side and back side heat transfer coefficient (HTC) are observed due to the geometrical pattern difference of the chevron plate heat exchanger [27]. The local condensation heat transfer coefficient reaches its maximum near the inlet port and minimum at the end faces on the left and right, attributed to refrigerant maldistribution, a phenomenon also evidenced by Longo et al [22]. The horizontal average condensation heat transfer coefficients for a mass flux of 10 kg/m²s are observed to decrease from about 2.7 to 1.5 kW/m²K with the increase of wetness i.e decrease of vapor quality from about 0.85 to 0.25 shown in Figure 4(f) due to the fact that lower vapor quality results in a thicker liquid film that reduces the heat transfer efficiency.

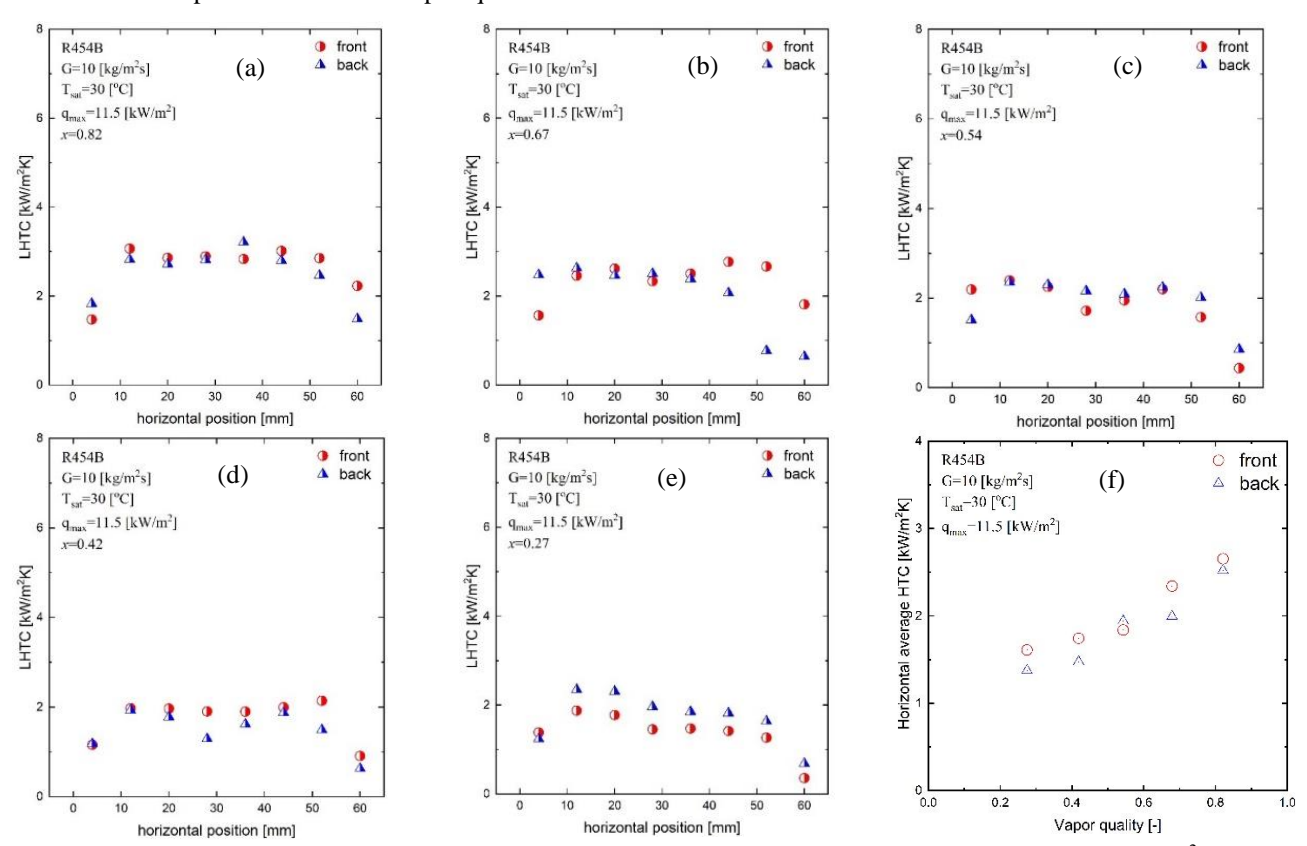


Figure 4: Condensation heat transfer coefficient of mixture refrigerant R454B for mass flux G=10 kg/m²s: (a)-(e) variation of local heat transfer coefficient with horizontal distance and (f) horizontal average heat transfer coefficient vs vapor quality.

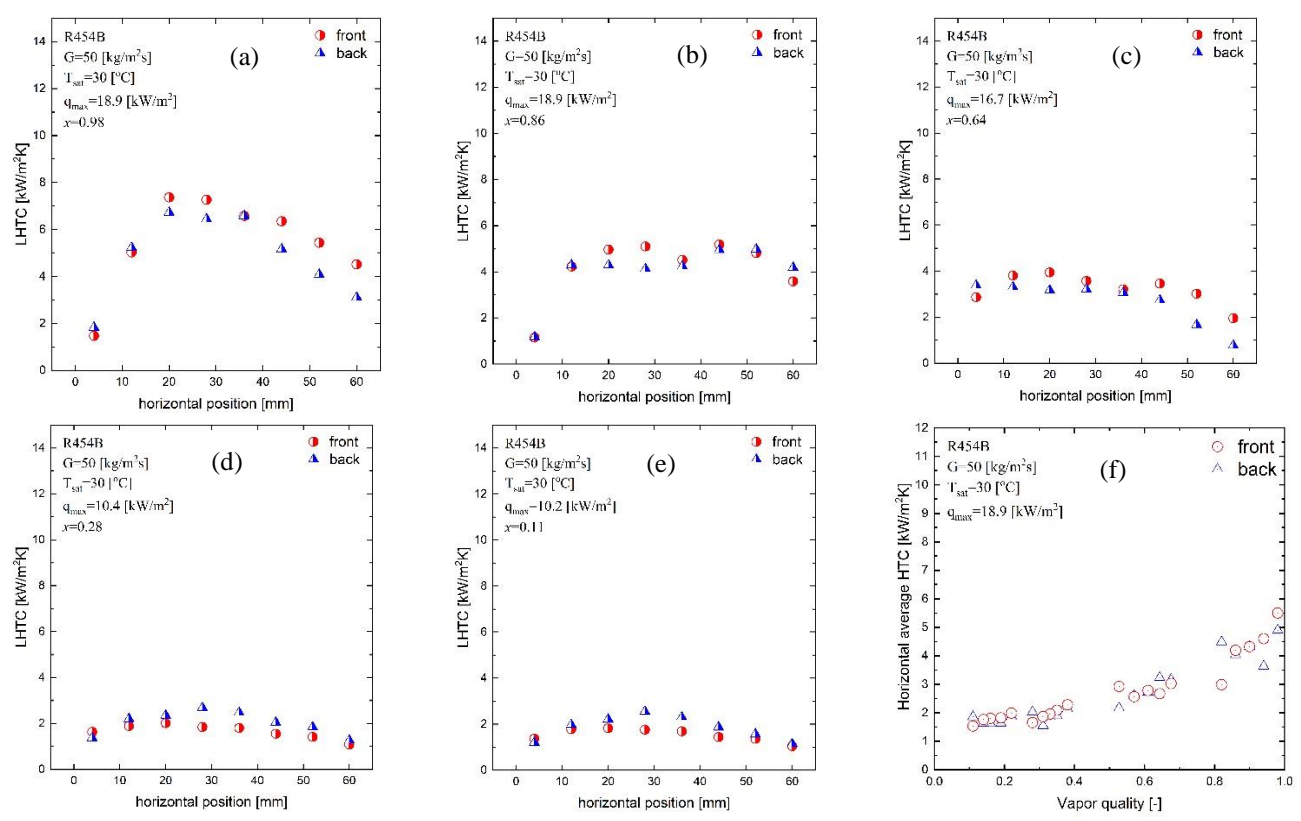


Figure 5: Condensation heat transfer coefficient of mixture refrigerant R454B for mass flux $G=50 \text{ kg/m}^2\text{s}$: (a) – (e) variation of local heat transfer coefficient with horizontal distance and (f) horizontal average heat transfer coefficient vs vapor quality

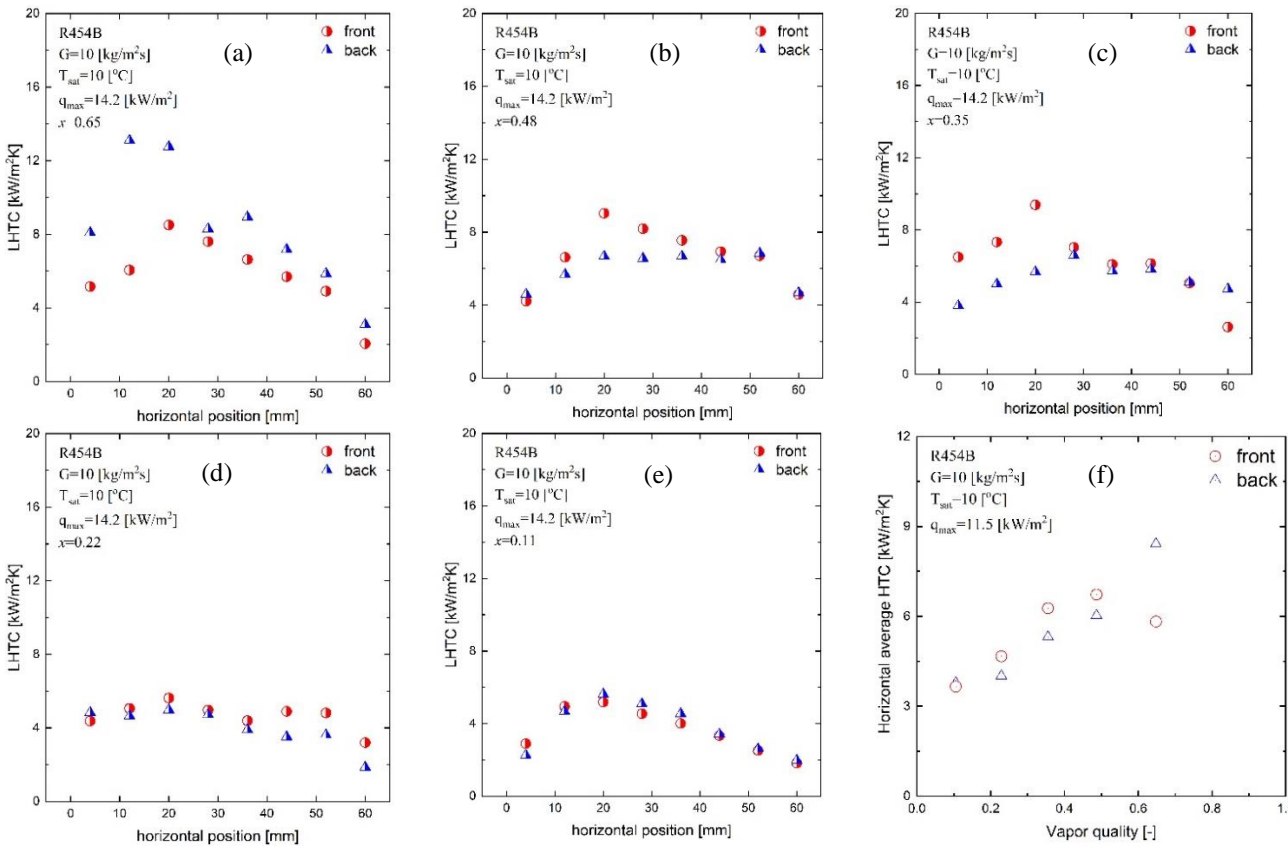


Figure 6: Evaporation heat transfer coefficient of mixture refrigerant R454B for mass flux $G=10 \text{ kg/m}^2\text{s}$: (a) – (e) variation of local heat transfer coefficient with horizontal distance and (f) horizontal average heat transfer coefficient vs vapor quality

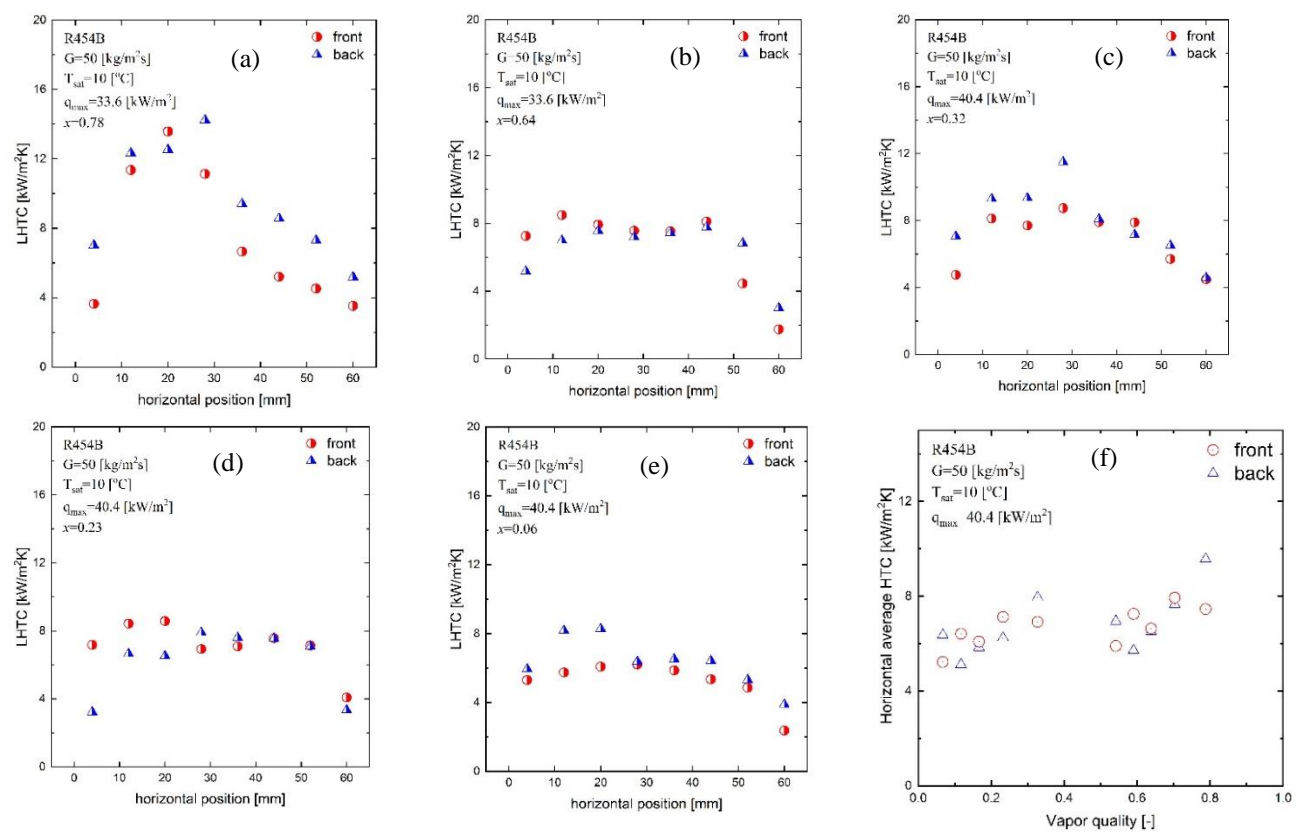


Figure 7: Evaporation heat transfer coefficient of mixture refrigerant R454B for mass flux $G=50 \text{ kg/m}^2\text{s}$: (a) – (e) variation of local heat transfer coefficient with horizontal distance and (f) horizontal average heat transfer coefficient vs vapor quality

From Figure 5(f), the horizontal average condensation HTC for a mass flux of $50 \text{ kg/m}^2\text{s}$ was found to decrease from $5.5 \text{ to } 1.5 \text{ KW/m}^2\text{K}$ with the decrease of vapor quality from 1.0 to 0.1. The elevated heat transfer coefficients observed at high vapor qualities (x>0.6) during the condensation experiment, particularly at a high mass flux of $50 \text{ kg/m}^2\text{s}$ in Figure 5(f), can be largely attributed to the substantial reduction in condensate film thickness. This thinning of the condensate film leads to a notable increase in the heat transfer coefficient.

From Figure 6(a), (b), (c), (d) and (e) and Figure 7(a), (b), (c), (d) and (e), greater zigzag patterns are evident in the trends of local evaporation heat transfer coefficient data during the evaporation of the mixture refrigerant R454B in the plate heat exchanger at mass fluxes of 10 kg/m²s and 50 kg/m²s. This behavior is attributed to increased turbulence and the intricate flow dynamics within the Plate Heat Exchanger (PHE). The local heat transfer coefficient values are observed to be higher in the middle section of the test plate due to the dominance of the convection boiling regime, particularly in the vapor-preferred pathway, as supported by the findings of Lee et al [18]. The horizontal average evaporation heat transfer coefficient for a mass flux of 10 kg/m²s are observed to increase from about 3.2 to 8.5 kW/m²K with the increase of vapor quality from about 0.10 to 0.72 shown in Figure 6(f) due to the fact that higher vapor quality results in a higher vapor velocity augmenting convective heat transfer through increased turbulence.

From Figure 7(f), the horizontal average evaporation HTC for a mass flux of 50 kg/m²s was found to increase from about 4.5 to 8.8 KW/m²K with the increase of vapor quality from 0.05 to 0.8. The evaporation heat transfer coefficient exhibits a significantly higher value at high vapor qualities (x > 0.5) and a high mass flux of 50 kg/m²s in Figure 7(f). This pronounced increase can be attributed to the increased turbulence and intricate flow dynamics prevalent under those specific test conditions.

The front side and back side horizontal average condensation heat coefficient for both mass fluxes of 10 kg/m²s and 50 kg/m²s do not have significant differences showing negligible effect of geometrical attributes of front side and back side of the plate heat exchanger with the only significant variation in horizontal distance as the results illustrated in Figure 4 and Figure 5. Furthermore, due to turbulence and flow behavior, the difference between the front side horizontal average evaporation heat transfer coefficient and back side horizontal average evaporation heat transfer coefficient observed in Figure 6 and Figure 7 are pronounced specially at high mass flux of 50 kg/m²s in comparison to lower mass flux of 10 kg/m²s signifying the effect of geometrical pattern of the front side and back side of the test plate. However, the effect of mass transfer resistance of mixture refrigerant R454B on local and average heat transfer coefficient in brazed type chevron plate heat exchanger are needed to be investigated in detail for understanding the heat transfer behavior of mixture refrigerant during condensation and evaporation.

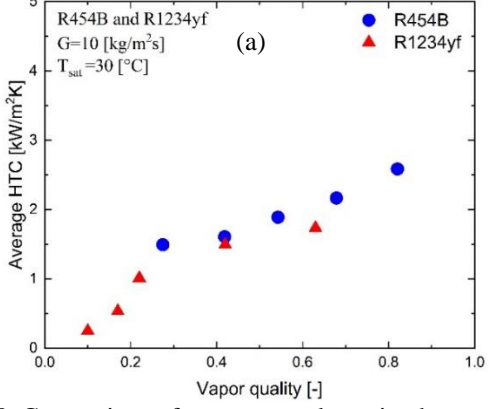
4.2 Comparison of heat transfer coefficient of R454B and R1234yf during condensation and evaporation

Figure 8 and Figure 9 show the comparison of experimentally measured average heat coefficients of R454B and R1234yf for mass flux of 10 kg/m²s and 50 kg/m²s during condensation and evaporation respectively. The average heat transfer coefficient is calculated by making average of previously obtained the front side horizontal average heat transfer coefficient and back side horizontal average heat transfer coefficient in the experiment. From Figure 8(a) and 8(b) it is observed that the average condensation heat transfer coefficient of both R454B and R1234yf decreases with increase of wetness (1-x) i.e. with decrease of vapor quality.

The low vapor quality in low mass flux results in thick condensate film that reduces the heat transfer coefficient in the test plate. The condensation heat transfer coefficient value for R454B is almost similar with R1234yf for vapor quality of x<0.4 at low mass flux of 10 kg/m²s and for vapor quality of x<0.5 at high mass flux of50 kg/m²s since the gravity controlled condensation dictates the condensation process, possibly showing negligible effect on heat transfer coefficient for both the R1234yf refrigerant and mixture refrigerant R454B (having constituents R1234yf) in this context. Moreover, the condensation heat transfer coefficient for R454B surpasses that of R1234yf at high vapor quality (x<0.7), especially

under larger mass flux conditions of 50 kg/m²s during forced convective condensation. This observation aligns with findings from another research group [30], which reported similar trends in their experimental study of condensation heat transfer in a microfin tube. The superior liquid thermal conductivity of R454B compared to R1234yf [29] can also contribute to the higher heat transfer coefficient exhibited by R454B relative to R1234yf. The average HTC of R454B increases from 1.5 to 5.0 kW/m²K and the average HTC of R1234yf increases from 0.8 to 3.1 kW/m²K when mass flux of 10 to 50 kg/m²s during the condensation heat transfer experiments around saturation temperature 30 °C.

From Figure 9(a) and 9(b) it is observed that the average evaporation heat transfer coefficient of both R454B and R1234yf increases with the increase of vapor quality. Since the heat transfer in the evaporation depends greatly on the flow pattern, increasing the mass flux creates more complex flow resulting the more zigzag trends in the heat transfer coefficients. Vertically across the plate, the heat transfer coefficients in the high vapor quality region are greater than those in the low vapor quality region. In evaporation process, in the higher vapor quality region, vapor specific volume increases, and the vapor velocity becomes faster at a given mass flux It is attributed that the velocity of vapor enhances the convection heat transfer since the turbulence level inside the plate heat exchanger increase. Moreover, the average HTC of R454B increases from 3.8 to 8.9 kW/m²K and the average HTC of R1234yf increases from 3.5 to 7.2 kW/m²K when mass flux of 10



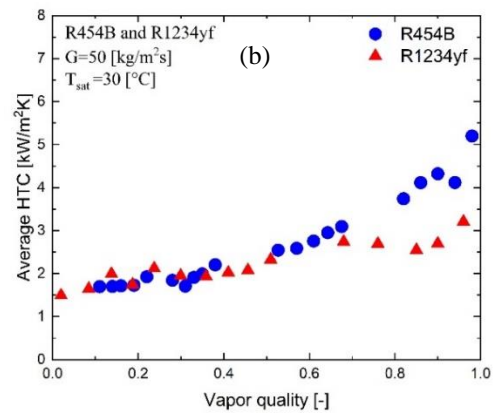
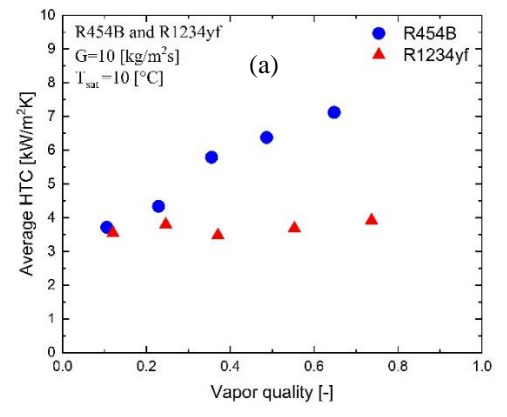


Figure 8: Comparison of average condensation heat transfer coefficients of R454B and R1234yf for mass flux (a) $G = 10 \text{ kg/m}^2\text{s}$ and (b) $G = 50 \text{ kg/m}^2\text{s}$.



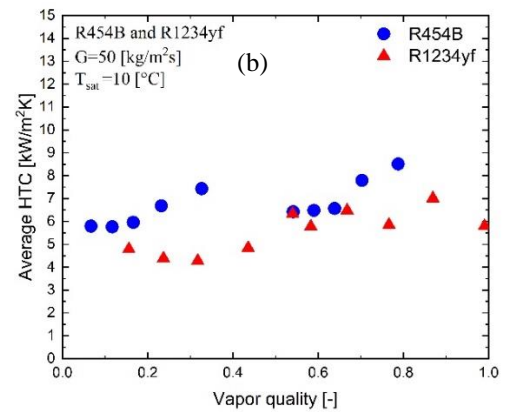


Figure 9: Comparison of average evaporation heat transfer coefficients of R454B and R1234yf for mass flux (a) $G = 10 \text{ kg/m}^2\text{s}$ and (b) $G=50 \text{ kg/m}^2\text{s}$.

to 50 kg/m²s during the evaporation heat transfer experiments around saturation temperature 10 °C. The evaporation heat transfer coefficient of R454B is also observed higher than that of R1234yf similar to condensation heat transfer coefficient results.

The heat transfer coefficients (HTCs) of R454B demonstrate a moderate improvement in comparison to R1234yf, showing an enhancement in the range of 1.1 to 1.7 times. This modest increase in HTCs is particularly noteworthy considering the composition of R454B, which includes a significant proportion of R32, accounting for approximately 68.9%. The limited growth in HTCs can be attributed to factors such as the influence of mass transfer resistance and the presence of a temperature glide within the zeotropic mixture refrigerant. These intricacies in composition contribute to a relatively subdued improvement in heat transfer performance for R454B when compared to R1234yf.

5. CONCLUSION

The local heat transfer coefficient of R454B (R32/R1234yf) were measured during condensation and evaporation in a vertical brazed plate heat exchanger. The experimental results for heat transfer can be summarized as follows:

- •The local heat transfer coefficient of R454B was found to vary both in flow direction in vertical cross section and width direction in horizontal distances of the plate. The maximum value was found near the inlet port because of inlet refrigerant distribution effect and also the tendency to flow the vapor preferred path.
- •The high heat transfer coefficients of R454B in the high vapor quality (x>0.6) at high mass flux of 50 kg/m²s in condensation experiment significantly attribute the condensate film thickness getting thinner results in an increase of heat transfer coefficient. The evaporation heat transfer coefficient of R454B in the high vapor quality (x>0.5) at high mass flux of 50 kg/m²s is much higher because of the more turbulence and complex flow at that test conditions.
- •The HTCs of R454B is moderately larger than R1234yf, increasing 1.1 to 1.7 times enhancement. HTC's growth is comparatively negligible, with R454B having a notable R32 composition of roughly 68.9% due to the deterioration of HTC caused by mass transfer resistance and the presence of a temperature glide of zeotropic mixture refrigerant.

ACKNOWLEDGEMENTS

The study was funded by New Energy and Industrial Technology Development Organization (NEDO), Japan. The author also would like to acknowledge Dr. ThihaTun, Mr. Kunpei Yoshida and Mr. Saide Diaw for their help and support in this work. We would like to acknowledge the presentation of the findings discussed in this paper at ISTP-33 (33rd International Symposium on Transport Phenomena) held in Kumamoto, Japan in September 24-27, 2023 where no formal proceedings were published.

NOMENCLATURE

Abbreviations

PHE	Plate Heat Exchanger
<i>BPHE</i>	Brazed Plate Heat Exchanger
GWP	Global Warming Potential
ODP	Ozone Depletion Potential
EU	European Union
HT	Heat Transfer
HTC	Heat Transfer Coefficient
LHTC	Local Heat Transfer Coefficient

Symbols

A: area	$[m^2]$
h: specific enthalpy	[J/kg]
Q: heat exchange amount	[kJ]
G: mass flux	$[kg/(m^2s]$
a: heat transfer coefficient	$[kW/(m^2 \cdot K]$
λ: thermal conductivity	$[kW/m \cdot K]$
x: vapor quality	[]
P: pressure	[MPa]
T: temperature	[°C]
q: heat flux	$[W/m^2]$
m: refrigerant mass flow rate	[kg/s]
W: mass fraction	[]
L: distance between thermocuples	[mm]

Subscripts

x: local point	l: liquid
w: water	v: vapor
r: refrigerant	p: plate

REFERENCES

- [1] D.H.Han, K.J. Lee and Y.H.Kim, "Experiments on the characteristics of evaporation of R410A in brazed plate heat exchangers with different geometric configurations". Applied Thermal Engineering 23 (10), 1209–1225.2003.
- [2] D.H. Han, K.J. Lee and Y.H. Kim, "The characteristics of condensation in brazed plate heat exchangers with different chevron angles". Journal of Korean Physics Sociecty, 43, 66–73, 2003.
- [3] Y.Y. Hsieh, and T.F. Lin , "Evaporation Heat Transfer and Pressure Drop of Refrigerant R-410A Flow in a Vertical Plate Heat Exchanger". Journal of Heat Transfer transactions of The ASME, 125, 852-857,2003.
- [4] A. Jokar, S.J.Eckels, M.H. Honsi, and T.P. Gielda, "Condensation heat transfer and pressure drop of brazed plate heat exchangers using refrigerant R-134a", Journal of Enhanced Heat Transfer, 11, 161–182.2004
- [5] W.S Kuo, Y.M. Lie, Y.Y.Hsieh, and T.F. Lin, "Condensation heat transfer and pressure drop of refrigerant R-410A flow in a vertical plate heat exchanger", International Journal of Heat and Mass Transfer48, 5205–5220,2005.
- [6] A. Jokar, M.H. Hosni and S.J. Eckels, "Dimensional analysis on the evaporation and condensation of refrigerant R-134a in minichannel plate heat exchangers", Applied Thermal Engineering ,26, 2287–2300, 2006.

- [7] J. Huang , T.J. Sheer and M. Bailey-McEwan "Heat transfer and pressure drop in plateheat exchanger refrigerant evaporators", International Journal of Refrigeration 35 325–335 .2012.
- [8] T.S. Khan, M.S. Khan, M.C. Chyu, and Z. H.Ayub, "Experimental investigation of evaporation heat transfer and pressure drop of ammonia in a 60° chevron plate heat exchanger", International Journal of Refrigeration 35 336–348, 2012.
- [9] T.S. Khan, M.S. Khan, M.C. Chyu, and Z. H.Ayub, "Evaporation heat transfer and pressure drop of ammonia in a mixed configuration chevron plate heat exchanger", International Journal of Refrigeration 41 92–102, 2014
- [10] B.H. Shon, S.W.Jeon, Y. Kim and Y.T. Kang, "Condensation and evaporation characteristics of low GWP refrigerants in plate heat exchangers", International Journal of Air-Conditioning and Refrigeration, 24(02), p.1630004.2016.
- [11] A. Desideri , J. Zhang , M. RyhlKærn , T. Ommen , J. Wronski , V. Lemort and F. Haglind, "An experimental analysis of flow boiling and pressure drop in a brazed plate heat exchanger for organic Rankine cycle power systems", International Journal of Heat and Mass Transfer113, 6–21 .96, 2017.
- [12] J. Zhang, A. Desideri, M. RyhlKærn, T. Ommen, J. Wronski and F. Haglind, "Flow boiling heat transfer and pressure drop characteristics of R134a, R1234yf and R1234ze in aplate heat exchanger for organic Rankine cycle units", International Journal of Heat and Mass Transfer 108 1787–1801,2017.
- $[13]\ M.\ Imran$, M. Usman , Y. Yang and B.S. Park, "Flow boiling of R245fa in the brazed plate heat exchanger: thermal and hydraulic performance assessment", International Journal of Heat and Mass Transfer 110 657-670,2017 .
- [14] B.H Shon, C.W.Jung, O.J. Kwon, C.K. Choi and Y.T. Kang, "Characteristics on condensation heat transfer and pressure drop for a low GWP refrigerant in brazed plate heat exchanger", International Journal of Heat and Mass Transfer 122, 1272–1282,2018.
- [15] E.M Djordjedvic, S. Kabelac, and S.P. Šerbanovic, "Mean heat transfer coefficient and pressure drop during the evaporation of 1,1,1,2 tetrafluoroethane (R-134a) in a plate heat exchanger", Journal of the Serbian Chemical Society72 833–846,2007.
- [16] E.M Djordjedvic, S. Kabelac, and S.P. Šerbanovic, "Heat transfer coefficient and pressure drop during refrigerant R134a condensation in a plate heat exchanger", Chemical Papers. 62 78–85,2008.
- [17] E.M. Djordjedvi and S. Kabelac, "Flow boiling of R134a and ammonia in a plate heat exchanger", International Journal of Heat Mass Transfer 51 6235–6242,2008 .
- [18] D.C. Lee , D. Kim , S. Park , J. Lim and Y. Kim, "Evaporation heat transfer coefficient and pressure drop of R-1233zd(E) in a brazed plate heat exchanger", Applied Thermal Engineering 130,1147–1155, 2018 .
- [19] K. Sarraf, S. Launay, G. El Achkar and L. Tadrist, "Local vs global heat transfer and flow analysis of hydrocarbon complete condensation in plate heat

- exchanger based on infrared thermography", International Journal of Heat Mass Transfer 90 878–893,2015 .
- [20] R. Wang, and S. Kabelac, "Condensation quasi-local heat transfer and frictional pres-sure drop of R1234ze(E) and R134a in a micro-structured plate heat exchanger", Applied Thermal Engineering 197, 117404,2021.
- [21] K.Kariya, M.S. Mahmud, A. Kawazoe and A. Miyara, "Local heat transfer characteristics of the R1234ze (E) two phase flow inside a plate heat exchanger". International Refrigeration and Air Conditioning Conference, West Lafayette, IA, USA, 11–14 July 2016; pp. 1–8,2016.
- [22] G.A. Longo, S. Mancin, G. Righetti, and C. Zilio, "Local heat transfer coefficients of R32 and R410a condensation inside a brazed plate heat exchanger (BPHE)". International Journal of Heat Mass Transfer, 194, 123041,2022.
- [23] M.S. Mahmud, K. Kariya and A. Miyara "Local Condensation Heat Transfer Characteristics of Refrigerant R1234ze(E) Flow Inside a Plate Heat Exchanger", International Journal of Air-Conditioning and Refrigeration, Vol. 25, 1750004,2017.
- [24] K. Kariya, and A. Miyara, "Condensation and evaporation heat transfer characteristics of pure and binary-mixture HFO refrigerants inside a plate heat exchanger". IIR International Congress of Refrigeration, Montréal, QC, Canada, 24–30 August 2019; pp. 1644–1651,2019.
- [25] T. Tun, K. Kariya and A. Miyara, "Consideration on local heat transfer measurement of plate heat exchanger with the aid of simulation", EPI International Journal of Engineering 3,1–9,2020.
- [26] M.M Rahman, T. Tun, K. Kariya and A. Miyara, "Experimental Study of Condensation Local Heat Transfer Characteristics of R454B in a Plate Heat Exchanger" JSRAE Annual Conference, Okayama, Japan, 2022
- [27] M.M. Rahman, D. Bal, K. Kariya and A. Miyara "Experimental analysis of local condensation heat transfer characteristics of CF_3I inside a plate heat exchanger", Fluids 8, no. 5: 150,2023.
- [28] D. Bal, M.M. Rahman, K. Kariya and A. Miyara, "Experimental study of evaporation local heat transfer characteristics of CF_3I in plate heat exchanger". International Heat Transfer Conference (IHTC), Cape town, South Africa, 2023
- [29] E. Lemmon, M.L. Huber and M.O. McLinden, NIST Standard Reference Database 23: Reference Fluid Thermodynamic and Transport Properties REFPROP, Version 10.0; Standard Reference Data Program; National Institute of Standards and Technology: Gaithersburg, MD, USA, 2018.
- [30] A.K Mainil, H. Ubudiyah ,N. Sakamoto, K. Kariya and A. Miyara, "Experimental Study on Condensation Heat Transfer of R454B inside Small Diameter Microfin Tube". International Refrigeration and Airconditioing Conference, Paper 2411 Purdue, USA, 2022.